

Abstracts

CATALYSIS – APPLIED AND PHYSICAL ASPECTS

Controlled Synthesis of Pt Nanoparticles *via* Seeding Growth and Their Shape-Dependent Catalytic Activity

X. Gong, Y. Yang, L. Zhang, C. Zou, P. Cai, G. Chen and S. Huang, *J. Colloid Interface Sci.*, 2010, **352**, (2), 379–385

Octahedral, cuboctahedral, branched and ‘rice-like’ Pt NPs were synthesised using a seed-mediated growth route. Pt NPs (3 nm) were prepared and dispersed in oleyl amine to form a seed solution and then Pt(acac)₂ was added. By adjusting the molar ratio of Pt from Pt(acac)₂ and seed NPs, the seed diameter and the addition route of Pt(acac)₂, the NPs growth could be controlled to fall into in a kinetic or thermodynamic growth regime. The obtained NPs were supported on C black (Vulcan XC-72). The catalysts synthesised from branched NPs were found to have higher catalytic activity and stability for the oxidation of methanol.

Pyrophoricity and Stability of Copper and Platinum Based Water-Gas Shift Catalysts during Oxidative Shut-Down/Start-Up

R. Kam, J. Scott, R. Amal and C. Selomulya, *Chem. Eng. Sci.*, 2010, **65**, (24), 6461–6470

In this investigation Cu/ZnO exhibited high levels of pyrophoricity. This manifested as a sharp temperature rise of the catalyst bed upon air introduction. Severe sintering of the bulk and metallic phases of the catalyst resulted in catalyst deactivation. No pyrophoricity was observed for Pt-based catalysts; however, there was sintering of the metallic phase in Pt/TiO₂ and Pt/ZrO₂. Pt/CeO₂ retained its activity, displaying no loss in specific surface area or metal dispersion.

Shape-Selective Formation and Characterization of Catalytically Active Iridium Nanoparticles

S. Kundu and H. Liang, *J. Colloid Interface Sci.*, 2011, **354**, (2), 597–606

Sphere, chain, flake and needle shaped Ir NPs were synthesised *via* reduction of Ir(III) ions in cetyltrimethylammonium bromide micellar media containing alkaline

2,7-dihydroxynaphthalene under UV irradiation. The NPs’ morphology was tuned by changing the surfactant:metal ion molar ratios and altering other parameters. The Ir nano-needles were a good catalyst for the reduction of organic dyes in presence of NaBH₄.

CATALYSIS – REACTIONS

Selective Oxidation of Glucose Over Carbon-Supported Pd and Pt Catalysts

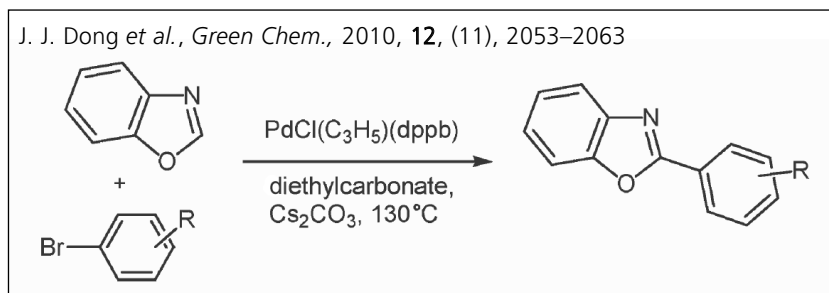
I. V. Delidovich, O. P. Taran, L. G. Matvienko, A. N. Simonov, I. L. Simakova, A. N. Bobrovskaya and V. N. Parmon, *Catal. Lett.*, 2010, **140**, (1–2), 14–21

Pt/C exhibited lower specific activity and provided poor selectivity of glucose oxidation to gluconic acid by O₂ in comparison with Pd/C. The finely dispersed Pd/C catalysts are prone to deactivation due to oxidation of their surface, while larger metal particles are more tolerant and stable. The activity of Pd nanoparticles can be maintained when the process is controlled by diffusion of O towards the active component of the catalyst.

Carbonates: Eco-Friendly Solvents for Palladium-Catalysed Direct Arylation of Heteroaromatics

J. J. Dong, J. Roger, C. Verrier, T. Martin, R. Le Goff, C. Hoarau and H. Doucet, *Green Chem.*, 2010, **12**, (11), 2053–2063

Direct 2-, 4- or 5-arylation of heteroaromatics with aryl halides using PdCl(C₃H₅)(dppb) as catalyst precursor/base was shown to proceed in moderate to good yields using the solvents diethylcarbonate (see the **Figure**) or propylene carbonate. The best yields were obtained using benzoxazole or thiazole derivatives (130°C). The arylation of furan, thiophene, pyrrole, imidazole or isoxazole derivatives was found to require a higher reaction temperature (140°C).



EMISSIONS CONTROL

A Global Description of DOC Kinetics for Catalysts with Different Platinum Loadings and Aging Status

K. Hauff, U. Tuttlies, G. Eigenberger and U. Nieken, *Appl. Catal. B: Environ.*, 2010, **100**, (1–2), 10–18

Five Pt/ γ -Al₂O₃ DOCs with different Pt loadings and ageing steps were characterised with regards to Pt particle diameter, active surface area and conversion behaviour for CO, propene and NO oxidation. HR-REM showed that the Pt particles have diameters larger than 8 nm. The catalyst activity was shown to be directly proportional to the catalytically active surface area, which was determined by CO chemisorption measurements. In order to model the CO and propene oxidation kinetics, only the catalytically active surface has to be changed in the global kinetic models. The same was true for NO oxidation at higher temperatures.

FUEL CELLS

High Platinum Utilization in Ultra-Low Pt Loaded PEM Fuel Cell Cathodes Prepared by Electro spraying

S. Martin, P. L. Garcia-Ybarra and J. L. Castillo, *Int. J. Hydrogen Energy*, 2010, **35**, (19), 10446–10451

The title cathodes with Pt loadings as low as 0.012 mg Pt cm⁻² were prepared by the electro spray method. SEM of these layers showed a high dispersion of the catalyst powders forming fractal deposits made by small clusters of Pt/C NPs, with the clusters arranging in a dendritic growth. Using these cathodes in MEAs, a high Pt utilisation in the range 8–10 kW g⁻¹ was obtained for a fuel cell operating at 40°C and atmospheric pressure. Moreover, a Pt utilisation of 20 kW g⁻¹ was attained at 70°C and 3.4 bar over-pressure.

Effect of MEA Fabrication Techniques on the Cell Performance of Pt–Pd/C Electrocatalyst for Oxygen Reduction in PEM Fuel Cell

S. Thanasilp and M. Hunsom, *Fuel*, 2010, **89**, (12), 3847–3852

The effect of three different MEA fabrication techniques: catalyst-coated substrate by direct spray (CCS), catalyst-coated membrane by direct spray (CCM-DS) or decal transfer (CCM-DT), on the O₂ reduction in a PEMFC was investigated under identical Pt-Pd/C loadings. The cells prepared by the CCM methods, and particularly by CCM-DT, exhibited a significantly higher open circuit voltage (OCV) but a

lower ohmic and charge transfer resistance. By using CV with H₂ adsorption, it was found that the electrochemically active area of the electrocatalyst prepared by CCM-DT was higher than those by CCS and CCM-DS. Under a H₂/O₂ system at 0.6 V, the cells with an MEA made by CCM-DT provided the highest cell performance (~350 mA cm⁻²).

METALLURGY AND MATERIALS

Shape Memory Effect and Pseudoelasticity of TiPt

Y. Yamabe-Mitarai, T. Hara, S. Miura and H. Hosoda, *Intermetallics*, 2010, **18**, (12), 2275–2280

Martensitic transformation behaviour and SM properties of Ti-50 at%Pt SMA were investigated using high-temperature XRD and loading–unloading compression tests. The structures of the parent and martensite phases were identified as B2 and B19, respectively. Strain recovery was observed during unloading at RT and at 1123 K, which was below the martensite temperature. Shape recovery was investigated for the samples by heating at 1523 K for 1 h. The strain recovery rate was 30–60% for the samples tested at RT and ~11% for the samples tested at 1123 K.

Role of Severe Plastic Deformation on the Cyclic Reversibility of a Ti_{50.3}Ni_{33.7}Pd₁₆ High Temperature Shape Memory Alloy

B. Kockar, K. C. Atli, J. Ma, M. Haouaoui, I. Karaman, M. Nagasako and R. Kainuma, *Acta Mater.*, 2010, **58**, (19), 6411–6420

The effect of microstructural refinement on the thermomechanical cyclic stability of the title HTSMA which was severely plastically deformed using equal channel angular extrusion (ECAE) was investigated. The grain/subgrain size of the high temperature austenite phase was refined down to ~100 nm. The increase in strength differential between the onset of transformation and the macroscopic plastic yielding after ECAE led to enhancement in the cyclic stability during isobaric cooling–heating. The reduction in irrecoverable strain levels is attributed to the increase in critical stress for dislocation slip due to the microstructural refinement during ECAE.

CHEMISTRY

The Chemistry of Tri- and High-Nuclearity Palladium(II) and Platinum(II) Complexes

V. K. Jain and L. Jain, *Coord. Chem. Rev.*, 2010, **254**, (23–24), 2848–2903

This review gives an overview of the title complexes and reports developments. Three or more square-planar metal atoms can be assembled in several ways resulting in complexes with a myriad of geometric forms. These square planes may be sharing a corner, an edge and two edges or even separated by ligands having their donor atoms incapable of forming chelates, yielding dendrimers and self-assembled molecules. Synthetic, spectroscopic and structural aspects of these complexes together with their applications are described. (Contains 554 references.)

ELECTRICAL AND ELECTRONICS

Dissolution and Interface Reactions between Palladium and Tin (Sn)-Based Solders:

Part I. 95.5Sn-3.9Ag-0.6Cu Alloy

P. T. Vianco, J. A. Rejent, G. L. Zender and P. F. Hlava, *Metall. Mater. Trans. A*, 2010, **41**, (12), 3042–3052

The interface microstructures and dissolution behaviour which occur between Pd substrates and molten 95.5Sn-3.9Ag-0.6Cu (wt%) were studied. The solder bath temperatures were 240–350°C, and the immersion times were 5–240 s. As a protective finish in electronic assemblies, Pd would be relatively slow to dissolve into molten Sn-Ag-Cu solder. The Pd-Sn intermetallic compound (IMC) layer would remain sufficiently thin and adherent to a residual Pd layer so as to pose a minimal reliability concern for Sn-Ag-Cu interconnections.

Dissolution and Interface Reactions between Palladium and Tin (Sn)-Based Solders:

Part II. 63Sn-37Pb Alloy

P. T. Vianco, J. A. Rejent, G. L. Zender and P. F. Hlava, *Metall. Mater. Trans. A*, 2010, **41**, (12), 3053–3064

The interface microstructures as well as the rate kinetics of dissolution and IMC layer formation were investigated for couples formed between molten 63Sn-37Pb (wt%) and Pd sheet. The solder bath temperatures were 215–320°C, and the immersion times were 5, 15, 30, 60, 120 and 240 s. The extents of Pd dissolution and IMC layer development were significantly greater for molten Sn-Pb than the Pb-free Sn-Ag-Cu (Part I, as above) at a given test temperature.

ELECTROCHEMISTRY

The Effect of Gold on Platinum Oxidation in Homogeneous Au–Pt Electrocatalysts

S. D. Wolter, B. Brown, C. B. Parker, B. R. Stoner and J. T. Glass, *Appl. Surf. Sci.*, 2010, **257**, (5), 1431–1436

Ambient air oxidation of Au-Pt thin films was carried out at RT and then the films were characterised by XPS. The homogeneous films were prepared by RF cosputtering with compositions varying from Au₉Pt₉₁ to Au₈₉Pt₁₁ and compared to pure Pt and Au thin films. The predominant oxidation products were PtO and PtO₂. Variations in Pt oxide phases and/or concentration did not contribute to enhanced electrocatalytic activity for oxygen reduction observed for the intermediate alloy stoichiometries.

A Feasibility Study of the Electro-recycling of Greenhouse Gases: Design and Characterization of a (TiO₂/RuO₂)/PTFE Gas Diffusion Electrode for the Electrosynthesis of Methanol from Methane

R. S. Rocha, L. M. Camargo, M. R. V. Lanza and R. Bertazzoli, *Electrocatalysis*, 2010, **1**, (4), 224–229

The title GDE was designed to be used in the electrochemical conversion of CH₄ into MeOH under conditions of simultaneous O₂ evolution. The GDE was prepared by pressing and sintering TiO₂(0.7)/RuO₂(0.3) powder and PTFE. CH₄ was inserted into the reaction medium by the GDE and electrosynthesis was carried out in 0.1 mol l⁻¹ Na₂SO₄. Controlled potential experiments showed that MeOH concentration increased with applied potential, reaching 220 mg l⁻¹ cm², at 2.2 V vs. a calomel reference electrode. Current efficiency for MeOH formation was 30%.

PHOTOCONVERSION

Cyclometalated Red Iridium(III) Complexes Containing Carbazolyl-Acetylacetonate Ligands: Efficiency Enhancement in Polymer LED Devices

N. Tian, Y. V. Aulin, D. Lenkeit, S. Pelz, O. V. Mikhnenko, P. W. M. Blom, M. A. Loi and E. Holder, *Dalton Trans.*, 2010, **39**, (37), 8613–8615

New red emitting cyclometalated Ir(III) complexes containing carbazolyl-acetylacetonate ligands (**1**, **2**) were prepared and then compared to the commonly used reference emitter [(btp)₂Ir(III)(acac)]. For a range of concentrations the new complexes revealed better luminous efficiencies than [(btp)₂Ir(III)(acac)]. The phosphorescence decay times of the newly designed triplet emitters are significantly shorter making them attractive candidates for applications in advanced organic and polymer LEDs.

N. Tian *et al.*, *Dalton Trans.*, 2010, **39**, (37), 8613–8615

